Acta Mech 228, 3511–3531 (2017)
DOI 10.1007/s00707-017-1888-2

ORIGINAL PAPER

D. V. Dung · Pham Minh Vuong

Analytical investigation on buckling and postbuckling of FGM toroidal shell segment surrounded by elastic foundation in thermal environment and under external pressure using TSDT

Received: 7 November 2016 / Revised: 8 April 2017 / Published online: 17 June 2017

Abstract In this paper, FGM toroidal shell segments surrounded by elastic foundation and subjected to uniform external pressure are investigated by analytical method. A novelty of the study is that the Reddy's third-order shear deformation shell theory (TSDT) with von Karman geometrical nonlinearity combined with deflection function selected with three terms is used to investigate the nonlinear stability of thicker FGM toroidal shell segments. In addition, the thermal element in the shell is also taken into account. The FGM shell is a convex and concave toroidal shell segment. It is a general form for a circular cylindrical shell. Closed-form expressions for determining the static critical external pressure load and postbuckling load–deflection curves are obtained. Effects of temperature field, foundations, material and dimensional parameters on the stability of shells are considered. This paper also shows that the use of TSDT to analyze the nonlinear stability of thicker toroidal shell segments is necessary and more suitable.

1 Introduction

Functionally graded material (FGM) is a material made of metal and ceramic. The highlights of FGM result from a combination of prominent characteristics of constituents such as high elasticity modulus, low thermal expansion and conduction coefficients of ceramic and ductility of metal. By gradually varying the volume fractions of constituent materials, the effective properties of an FGM exhibit a smooth and continuous change from one surface to another, thus reducing or eliminating interface bond problems and huge stress concentration that are inherent in laminated composites. In recent years, FGM structures are used efficiently in various engineering applications as pressure vessels, missiles, spacecraft, submarines and nuclear reactors.

Due to the importance of FGM structures in practical applications, studies on the static and dynamic behavior of FGM structures have attracted attention of many scientists. Many significant results have been obtained. Batra [1] investigated the torsion of un-stiffened cylinders with material modulus varying only in the axial direction. Wang et al. [2] presented an exact solution and transient behavior for torsional vibration of functionally graded finite hollow cylinder. Shen [3] based on the higher-order shear deformation theory and the singular perturbation technique obtained results on torsional loads and the postbuckling equilibrium paths of torsion-loaded FGM shells in thermal environments. Huang and Han [4–7], with the three-term deflection function, analyzed the buckling and postbuckling of un-stiffened FGM cylindrical shells under axial compressive load, radial pressure and combined axial compressive load and radial pressure based on the

D. V. Dung
Department of Mathematics - Mechanics and Informatics, Vietnam National University, Hanoi, Vietnam

P. M. Vuong (✉)
Faculty of Civil and Industrial, National University of Civil Engineering, Hanoi, Vietnam
E-mail: phamminhvuongkhtn@gmail.com
Tel.: +84 963424199

Donnell shell theory with the von Karman geometrical nonlinearity and Ritz method. By the same authors, the nonlinear dynamic buckling problems of un-stiffened functionally graded cylindrical shells subjected to time-dependent axial load by using the one-term solution form is investigated [8]. Various effects of the inhomogeneous parameter, loading speed, dimension parameters, environmental temperature rise and initial geometrical imperfection on nonlinear dynamic buckling were discussed in their works.

Sofiyev and Schnack [9] investigated the stability of un-stiffened FGM cylindrical shells under linearly increasing dynamic torsional loading. The modified Donnell-type dynamic stability equation and Galerkin method were used. However, the geometrical relation is linear and the approximate solution was chosen by one term. Najafizadeh et al. [10] with the linear stability equations in terms of displacements studied buckling of FGM cylindrical shell reinforced by FGM rings and stringers under axial compression. By homogeneous reinforcement stiffeners, Bich et al. [11,12] have obtained the results on the nonlinear static and dynamic analysis of stiffened FGM imperfect doubly curved thin shallow shells and stiffened FGM cylindrical shells using the classical shell theory with von Karman geometrical nonlinearity and the smeared stiffeners technique. The nonlinear critical dynamic buckling load is found according to the Budiansky–Roth criterion. Dung and Hoa [13,14] obtained the results on the nonlinear static buckling and postbuckling analysis of eccentrically stiffened FGM circular cylindrical shells under torsional and external loads without taking into account thermal elements.

For shells resting on elastic foundations, many investigations have focused on the buckling and postbuckling analysis of un-stiffened shells. Sheng and Wang [15] considered the effect of thermal load on buckling, vibration and dynamic buckling of un-stiffened FGM cylindrical shells embedded in a linear elastic medium based on the first-order shear deformation theory (FSDT) taking into account the rotary inertia and transverse shear strains. Shen [16] and Shen et al. [17] presented the postbuckling analysis of FGM cylindrical shells surrounded by an elastic medium under the lateral pressure and axial load by using the singular perturbation technique and the higher-order shear deformation shell theory (HDST). Sofiyev and Avcar [18] studied the stability of cylindrical shells containing an FGM layer subjected to axial load on the Pasternak foundation by the Galerkin method. By the same method, Sofiyev and Kuruoglu [19] analyzed the torsional vibration and buckling of the un-stiffened cylindrical shell with functionally graded coatings surrounded by an elastic medium. Najafov et al. [20] studied torsional vibration and stability of functionally graded orthotropic cylindrical shells on elastic foundation using the classical shell theory and Galerkin method. Bagherizadeh et al. [21] based on the higher-order shear deformation shell theory investigated the mechanical buckling of FGM cylindrical shells surrounded by a Pasternak elastic foundation. Akbari et al. [22] studied the thermal buckling of temperature-dependent FGM conical shells with arbitrary edge supports by an iterative generalized differential quadrature method. Bich and Tung [23] presented an analytical approach to investigate nonlinear axisymmetric responses of FGM shallow spherical shells under uniform external pressure including temperature effects using the classical shell theory. Dung and Nam [24], by semi-analytical approach, presented the nonlinear dynamic analysis of eccentrically stiffened functionally graded circular cylindrical thin shells under pressure and surrounded by an elastic medium without taking into account thermal elements.

For shells of revolution and toroidal shells, many interesting results on vibration and stability have been obtained. Stein and McElman [25] studied static buckling of isotropic shallow segment of toroidal shell. Hutchinson [26] analyzed initial postbuckling behavior of toroidal shell segments. Parnell [27] reported a numerical improvement of asymptotic solutions for shells of revolution with application to toroidal shell segments. Using the theory of thin shells for deriving inhomogeneous Heun equations in complex form, Guodong [28] presented exact solutions of toroidal shells in pressure vessels and piping under symmetric load. Wang Anwen and Zhang Wei [29], by asymptotic solution, solved the problem on the buckling of toroidal shells subjected to hydrostatic pressure based on Sander nonlinear equations of equilibrium. Zhang [30], based on Novozhilov thin shell equations, presented the complete asymptotic expansions of four homogeneous solutions and a particular solution of toroidal shells under nonsymmetric loadings. Zhu [31] studied the vibration and stability of toroidal shells conveying fluid by the use of Love general thin shell equations and the classical flow theory. A general solution for the natural frequency is obtained in that work. Blachut and Jaiswal [32], by numerical method, investigated the elastic and elastic-plastic buckling of geometrically perfect and imperfect toroidal shells under uniform external pressure. The geometrically nonlinear problems of in-plane pure bending of a toroidal shell of arbitrary cross section are considered by Kuznetsov and Levyakov [33]. A finite element algorithm for solution of the problem is proposed in their work. The free vibrations of elastic in vacuo circular toroidal shells under different boundary conditions are studied by Ming et al. [34] using the Sander linear thin shell theory. Buchanan and Liu [35] investigated the free vibration of thick-walled isotropic toroidal shells by the finite element method in which the nine-node Lagrangian finite element is formulated in the toroidal

coordinate system. Solutions are obtained for the case where an axis of symmetry can be assumed at the center of the torus. Asratyan and Gevorgyan[36] solved mixed boundary-value problems of thermoelasticity for anisotropic-in-plan inhomogeneous toroidal shells by asymptotic integration of the equations of the three-dimensional problem of the anisotropic shell theory. Using the first-order shear deformation theory, Tornabene and Viola [37] presented the static analysis of FGM doubly curved shells and panels of revolution by the generalized differential quadrature method. Bich et al. [38] studied the buckling of eccentrically stiffened functionally graded toroidal shell segment surrounded by an elastic medium under external pressure based on the classical thin shell theory.

To the best of the authors' knowledge, there is no analytical approach on the nonlinear buckling of FGM toroidal shell segments subjected to external pressure using TSDT. This problem has attracted the attention of many scientists, because studies [25–27,38] using the classical theory are only suitable for thin shells. For thicker shells, one must use the first-order shear deformation theory (FSDT) or the third-order shear deformation theory (TSDT) for better results. However, according to TSDT, the system stable equations will be the system of interdependent five equations, more complex than the system stable equations of the classical theory having only three equations. In this paper, the mentioned difficulty will be over come. In addition, this problem is complicated further if deflection function is selected with three terms. A novelty of this study is the use of TSDT combined with deflection function selected with three terms to investigate the nonlinear stability of FGM thicker toroidal shell segments.

In this paper, FGM thick toroidal shell segments surrounded by elastic foundation and subjected to uniform external pressure are considered, based on the Reddy's third-order shear deformation shell theory. The deflection function with three terms taking into account the nonlinear buckling shape is chosen more correctly and satisfying simply supported boundary conditions at the butt-ends of the shell. By using Galerkin's method, the closed-form expressions to determine critical buckling load and nonlinear postbuckling load–deflection curves are obtained. The influences of various parameters such as temperature field, radius of longitudinal curvature, foundation, dimensional parameters and volume fraction index of materials on the nonlinear behavior of the shell are analyzed.

2 Governing equations

2.1 Functionally graded material (FGM)

FGMs are microscopically inhomogeneous materials, in which material properties vary smoothly and continuously from one surface to the other structure surface. These materials are made from a mixture of ceramic and metal or a combination of different materials. In particular, FGM thin-walled structures with ceramic in the inner surface and metal in the outer surface are widely used in practice. Denote by V_{m} and V_{c} volume fractions of metal and ceramic phases, respectively, which are related by $V_{\mathrm{m}} + V_{\mathrm{c}} = 1$ and V_{c} is expressed as $V_{\mathrm{c}}(z) = (\frac{2z+h}{2h})^k$, where h is the thickness of thin-walled structure, k is the volume fraction exponent ($k \geq 0$); z is the thickness coordinate and varies from $-h/2$ to $h/2$; the subscripts m and c refer to the metal and ceramic constituents, respectively. According to the mentioned law, the Young's modulus $E(z)$ and the thermal expansion coefficient $\alpha(z)$ can be expressed in the form [10,13,39,40]

$$\begin{aligned} E(z) &= E_{\mathrm{m}} V_{\mathrm{m}} + E_{\mathrm{c}} V_{\mathrm{c}} = E_{\mathrm{m}} + (E_{\mathrm{c}} - E_{\mathrm{m}}) \left(\frac{2z+h}{2h} \right)^k, \\ \alpha(z) &= \alpha_{\mathrm{m}} V_{\mathrm{m}} + \alpha_{\mathrm{c}} V_{\mathrm{c}} = \alpha_{\mathrm{m}} + (\alpha_{\mathrm{c}} - \alpha_{\mathrm{m}}) \left(\frac{2z+h}{2h} \right)^k. \end{aligned} \tag{1}$$

The Poisson's ratio ν is assumed to be constant.

2.2 Constitutive relations and governing equations

Assume there is a plane circular arc of radius a (Fig. 1a, b). Rotating this arc about an axis orthogonal to equator line in their plane, we obtain the middle surface of a shell of revolution called a segment of toroidal shell. If the curvature $1/a$ is positive, this shell is a convex shell (Fig. 1c), but if $1/a$ is negative, this shell is a concave shell, if $1/a \to 0$, the shell becomes a cylindrical shell.

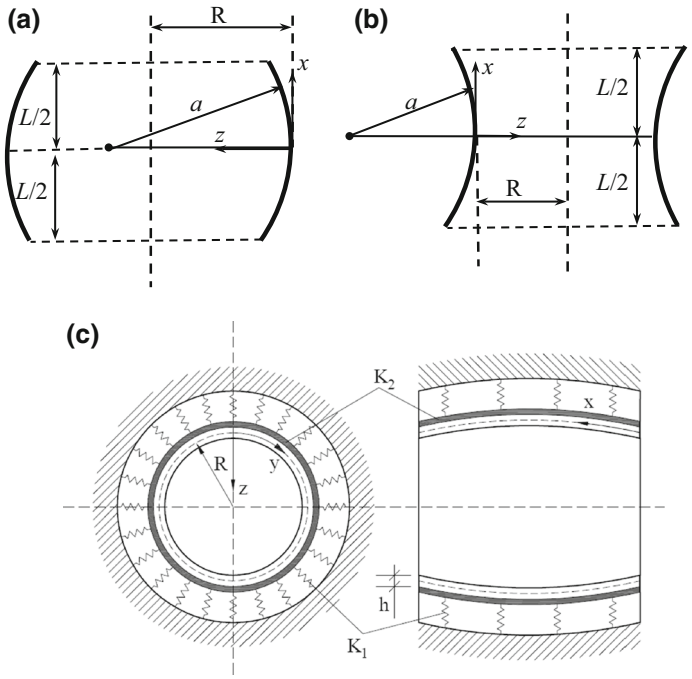

Fig. 1 Geometry and coordinate system of a FGM toroidal shell segment

Now consider a segment of toroidal shell formed as was said above and has the thickness h, length L, radius of shell equator R. The geometry and coordinate system of FGM toroidal shell segments are depicted in Fig. 1. In this paper, the FGM toroidal shell segments are free and are simply supported at two end edges and subjected to uniform external pressure.

The shell–foundation interaction is represented by the Pasternak model as [41]

$$q_{\mathrm{sf}} = K_1 w - K_2 \Delta w, \tag{2}$$

where K_1 is the Winkler foundation modulus and K_2 is the shear layer foundation stiffness of the Pasternak model, w is the deflection of the shell, and Δ is the Laplace operator.

According to the Reddy's third-order shear deformation shell theory, the displacement field at a distance z from the middle surface is as [40]

$$\begin{pmatrix} \overline{u} \\ \overline{v} \\ \overline{w} \end{pmatrix} = \begin{pmatrix} u + z\phi_x - \frac{4}{3h^2} z^3 (\phi_x + w_{,x}) \\ v + z\phi_y - \frac{4}{3h^2} z^3 (\phi_y + w_{,y}) \\ w \end{pmatrix}, \tag{3}$$

where u, v and w are the displacement components at the middle surface and ϕ_x, ϕ_y are the slope rotations in the (x, z) and (y, z) planes.

The strain components at the middle surface of toroidal shell segment are related to the displacements u, v and w in the x, y, z coordinate directions as [25,26,40]

$$\begin{pmatrix} \varepsilon_x^0 \\ \varepsilon_y^0 \\ \gamma_{xy}^0 \end{pmatrix} = \begin{pmatrix} u_{,x} - \frac{w}{a} + w_{,x}^2/2 \\ v_{,y} - \frac{w}{R} + w_{,y}^2/2 \\ u_{,y} + v_{,x} + w_{,x} w_{,y} \end{pmatrix}. \tag{4}$$

The strain components across the shell thickness at a distance z from the middle surface are

$$\begin{pmatrix} \varepsilon_x \\ \varepsilon_y \\ \gamma_{xy} \end{pmatrix} = \begin{pmatrix} \varepsilon_x^0 \\ \varepsilon_y^0 \\ \gamma_{xy}^0 \end{pmatrix} + z \begin{pmatrix} k_x^{(1)} \\ k_y^{(1)} \\ k_{xy}^{(1)} \end{pmatrix} + z^3 \begin{pmatrix} k_x^{(3)} \\ k_y^{(3)} \\ k_{xy}^{(3)} \end{pmatrix}, \begin{pmatrix} \gamma_{xz} \\ \gamma_{yz} \end{pmatrix} = \begin{pmatrix} \gamma_{xz}^0 \\ \gamma_{yz}^0 \end{pmatrix} + z^2 \begin{pmatrix} k_{xz}^{(2)} \\ k_{yz}^{(2)} \end{pmatrix}, \tag{5}$$

where

$$\begin{pmatrix} k_x^{(1)} \\ k_y^{(1)} \\ k_{xy}^{(1)} \end{pmatrix} = \begin{pmatrix} \phi_{x,x} \\ \phi_{y,y} \\ \phi_{x,y} + \phi_{y,x} \end{pmatrix}, \begin{pmatrix} k_{xz}^{(2)} \\ k_{yz}^{(2)} \end{pmatrix} = -3c \begin{pmatrix} \phi_x + w_{,x} \\ \phi_y + w_{,y} \end{pmatrix},$$
$$\begin{pmatrix} k_x^{(3)} \\ k_y^{(3)} \\ k_{xy}^{(3)} \end{pmatrix} = -c \begin{pmatrix} \phi_{x,x} + w_{,xx} \\ \phi_{y,y} + w_{,yy} \\ \phi_{x,y} + \phi_{y,x} + 2w_{,xy} \end{pmatrix}, \begin{pmatrix} \gamma_{xz}^0 \\ \gamma_{yz}^0 \end{pmatrix} = \begin{pmatrix} \phi_x + w_{,x} \\ \phi_y + w_{,y} \end{pmatrix}, c = \frac{4}{3h^2}. \tag{6}$$

From Eq. (4), the deformation compatibility equation for a toroidal shell segment is written as follows:

$$\varepsilon_{x,yy}^0 + \varepsilon_{y,xx}^0 - \gamma_{xy,xy}^0 = -\frac{1}{R} w_{,xx} - \frac{1}{a} w_{,yy} + (w_{,xy})^2 - w_{,xx} w_{,yy}. \tag{7}$$

The constitutive stress–strain equations by Hooke's law for the shell material are given by

$$\begin{pmatrix} \sigma_x \\ \sigma_y \end{pmatrix} = \frac{E(z)}{1-\nu^2} \begin{pmatrix} \varepsilon_x + \nu\varepsilon_y - (1+\nu)\alpha(z)\Delta T \\ \varepsilon_y + \nu\varepsilon_x - (1+\nu)\alpha(z)\Delta T \end{pmatrix},$$
$$\begin{pmatrix} \sigma_{xy} \\ \sigma_{xz} \\ \sigma_{yz} \end{pmatrix} = \frac{E(z)}{2(1+\nu)} \begin{pmatrix} \gamma_{xy} \\ \gamma_{xz} \\ \gamma_{yz} \end{pmatrix}, \tag{8}$$

where ΔT is temperature rise from stress-free initial state or temperature difference between two surfaces of the FGM shell.

The middle surface normal force intensities N_i, the bending moment intensities M_i and higher-order bending moment intensities P_i, transverse shearing force intensities Q_i and the higher-order shear force intensities R_i of functionally graded toroidal shell segment are defined as

$$N_i = \int_{-h/2}^{h/2} \sigma_i \mathrm{d}z,\ M_i = \int_{-h/2}^{h/2} z\sigma_i \mathrm{d}z,\ P_i = \int_{-h/2}^{h/2} z^3\sigma_i \mathrm{d}z,\ Q_i = \int_{-h/2}^{h/2} \sigma_{iz} \mathrm{d}z,$$
$$R_i = \int_{-h/2}^{h/2} z^2\sigma_{iz} \mathrm{d}z,\ N_{xy} = \int_{-h/2}^{h/2} \sigma_{xy} \mathrm{d}z,\ M_{xy} = \int_{-h/2}^{h/2} z\sigma_{xy} \mathrm{d}z,\ P_{xy} = \int_{-h/2}^{h/2} z^3\sigma_{xy} \mathrm{d}z, \tag{9}$$
$$i = x, y.$$

Integrating the stress–strain equations and their moments through the thickness of the shell, the expressions for force and moment resultants of a FGM toroidal shell segment are obtained as follows:

$$\begin{aligned} N_x &= \frac{E_1}{1-\nu^2}\left(\varepsilon_x^0 + \nu\varepsilon_y^0\right) + \frac{E_2}{1-\nu^2}(\phi_{x,x} + \nu\phi_{y,y}) - \frac{cE_4}{1-\nu^2}(\phi_{x,x} + w_{,xx} + \nu\phi_{y,y} + \nu w_{y,y}) - \frac{\Phi_1}{1-\nu}, \\ N_y &= \frac{E_1}{1-\nu^2}\left(\varepsilon_y^0 + \nu\varepsilon_x^0\right) + \frac{E_2}{1-\nu^2}(\phi_{y,y} + \nu\phi_{x,x}) \\ &\quad - \frac{cE_4}{1-\nu^2}(\phi_{y,y} + w_{,yy} + \nu\phi_{x,x} + \nu w_{x,x}) - \frac{\Phi_1}{1-\nu}, \\ N_{xy} &= \frac{E_1}{2(1+\nu)}\gamma_{xy}^0 + \frac{E_2}{2(1+\nu)}(\phi_{x,y} + \phi_{y,x}) - \frac{cE_4}{2(1+\nu)}(\phi_{x,y} + \phi_{y,x} + 2w_{,xy}), \end{aligned} \tag{10}$$

$$\begin{aligned} M_x &= \frac{E_2}{1-\nu^2}\left(\varepsilon_x^0 + \nu\varepsilon_y^0\right) + \frac{E_3}{1-\nu^2}(\phi_{x,x} + \nu\phi_{y,y}) - \frac{cE_5}{1-\nu^2}(\phi_{x,x} + w_{,xx} + \nu\phi_{y,y} + \nu w_{y,y}) - \frac{\Phi_2}{1-\nu}, \\ M_y &= \frac{E_2}{1-\nu^2}\left(\varepsilon_y^0 + \nu\varepsilon_x^0\right) + \frac{E_3}{1-\nu^2}(\phi_{y,y} + \nu\phi_{x,x}) \\ &\quad - \frac{cE_5}{1-\nu^2}(\phi_{y,y} + w_{,yy} + \nu\phi_{x,x} + \nu w_{x,x}) - \frac{\Phi_2}{1-\nu}, \\ M_{xy} &= \frac{E_2}{2(1+\nu)}\gamma_{xy}^0 + \frac{E_3}{2(1+\nu)}(\phi_{x,y} + \phi_{y,x}) - \frac{cE_5}{2(1+\nu)}(\phi_{x,y} + \phi_{y,x} + 2w_{,xy}), \end{aligned} \tag{11}$$

$$
\begin{aligned}
P_x &= \frac{E_4}{1-\nu^2}\left(\varepsilon_x^0+\nu\varepsilon_y^0\right)+\frac{E_5}{1-\nu^2}(\phi_{x,x}+\nu\phi_{y,y})-\frac{cE_7}{1-\nu^2}(\phi_{x,x}+w_{,xx}+\nu\phi_{y,y}+\nu w_{y,y})-\frac{\Phi_4}{1-\nu},\\
P_y &= \frac{E_4}{1-\nu^2}\left(\varepsilon_y^0+\nu\varepsilon_x^0\right)+\frac{E_5}{1-\nu^2}(\phi_{y,y}+\nu\phi_{x,x})\\
&\quad-\frac{cE_7}{1-\nu^2}(\phi_{y,y}+w_{,yy}+\nu\phi_{x,x}+\nu w_{x,x})-\frac{\Phi_4}{1-\nu},\\
P_{xy} &= \frac{E_4}{2(1+\nu)}\gamma_{xy}^0+\frac{E_5}{2(1+\nu)}(\phi_{x,y}+\phi_{y,x})-\frac{cE_7}{2(1+\nu)}(\phi_{x,y}+\phi_{y,x}+2w_{,xy}),
\end{aligned}
\tag{12}
$$

$$
\begin{aligned}
Q_x &= \frac{E_1-3cE_3}{2(1+\nu)}(\phi_x+w_{,x}),\ Q_y=\frac{E_1-3cE_3}{2(1+\nu)}(\phi_y+w_{,y}),\\
R_x &= \frac{E_3-3cE_5}{2(1+\nu)}(\phi_x+w_{,x}),\ R_y=\frac{E_3-3cE_5}{2(1+\nu)}(\phi_y+w_{,y}),
\end{aligned}
\tag{13}
$$

where

$$
\begin{aligned}
E_1 &= E_{\mathrm{m}}h+\frac{E_{cm}h}{k+1},\ E_2=\frac{E_{cm}kh^2}{2(k+1)(k+2)},\ E_3=\frac{E_{\mathrm{m}}h^3}{12}+E_{cm}h^3\left[\frac{1}{k+3}-\frac{1}{k+2}+\frac{1}{4(k+1)}\right],\\
E_4 &= E_{cm}h^4\left[\frac{1}{k+4}-\frac{3}{2(k+3)}+\frac{3}{4(k+2)}-\frac{1}{8(k+1)}\right],\\
E_5 &= \frac{E_{\mathrm{m}}h^5}{80}+E_{cm}h^5\left[\frac{1}{k+5}-\frac{2}{k+4}+\frac{3}{2(k+3)}-\frac{1}{2(k+2)}+\frac{1}{16(k+1)}\right],\\
E_7 &= \frac{E_{\mathrm{m}}h^7}{448}+E_{cm}h^7\left[\frac{1}{k+7}-\frac{3}{k+6}+\frac{15}{4(k+5)}-\frac{5}{2(k+4)}+\frac{15}{16(k+3)}-\frac{3}{16(k+2)}+\frac{1}{64(k+1)}\right],
\end{aligned}
\tag{14}
$$

$$
\begin{aligned}
\Phi_1 &= \int_{-h/2}^{h/2} E(z)\alpha(z)\Delta T(z)\mathrm{d}z,\\
\Phi_2 &= \int_{-h/2}^{h/2} zE(z)\alpha(z)\Delta T(z)\mathrm{d}z,\\
\Phi_4 &= \int_{-h/2}^{h/2} z^3E(z)\alpha(z)\Delta T(z)\mathrm{d}z.
\end{aligned}
\tag{15}
$$

If $\Delta T=\text{const}$, then

$$
\begin{aligned}
&\Phi_1=\Phi_{10}\Delta T;\ \textit{where}\ \Phi_{10}=\left(E_{\mathrm{m}}\alpha_{\mathrm{m}}+\frac{E_{\mathrm{m}}\alpha_{cm}+E_{cm}\alpha_{\mathrm{m}}}{k+1}+\frac{E_{cm}\alpha_{cm}}{2k+1}\right)h,\\
&\Phi_2=\left(\frac{E_{\mathrm{m}}\alpha_{cm}+E_{cm}\alpha_{\mathrm{m}}}{k+2}+\frac{E_{cm}\alpha_{cm}}{2k+1}\right)\frac{kh^2\Delta T}{2(k+1)},\\
&\Phi_4=\left[\frac{(k^2+3k+8)(E_{\mathrm{m}}\alpha_{cm}+E_{cm}\alpha_{\mathrm{m}})}{(k+3)(k+4)}+\frac{(2k^2+3k+4)E_{cm}\alpha_{cm}}{(2k+1)(2k+3)}\right]\frac{kh^4\Delta T}{8(k+1)(k+2)}.
\end{aligned}
\tag{16}
$$

According to the Reddy's third-order shear deformation theory, the nonlinear equilibrium equations of a toroidal shell segment under external pressure $q(\mathrm{N/m^2})$ surrounded by elastic foundation are of the form [40]

$$
\begin{aligned}
&N_{x,x}+N_{xy,y}=0,\\
&N_{xy,x}+N_{y,y}=0,
\end{aligned}
\tag{17.1}
$$

$$
\begin{aligned}
&Q_{x,x}+Q_{y,y}-3c(R_{x,x}+R_{y,y})+c(P_{x,xx}+2P_{xy,xy}+P_{y,yy})+\frac{1}{R}N_y+\frac{1}{a}N_x\\
&\quad+N_xw_{,xx}+2N_{xy}w_{,xy}+N_yw_{,yy}+q-K_1w+K_2(w_{,xx}+w_{,yy})=0,
\end{aligned}
\tag{17.2}
$$

$$M_{x,x} + M_{xy,y} - Q_x + 3cR_x - c(P_{x,x} + P_{xy,y}) = 0, \tag{17.3}$$
$$M_{y,y} + M_{xy,x} - Q_y + 3cR_y - c(P_{y,y} + P_{xy,x}) = 0, \tag{17.4}$$

where $K_1(\mathrm{N/m^3})$ is the linear stiffness of the foundation, and $K_2(\mathrm{N/m})$ is the shear modulus of the subgrade.

By introducing a stress function $F(x, y)$ as

$$N_x = F_{,yy}, N_y = F_{,xx}, N_{xy} = -F_{,xy}, \tag{18}$$

it is obvious that Eqs. (17.1) are identically satisfied.

The reverse relations are obtained from Eq. (10):

$$\begin{aligned}
\varepsilon_x^0 &= \frac{F_{,yy} - \nu F_{,xx}}{E_1} - \frac{E_2}{E_1}\phi_{x,x} + \frac{cE_4}{E_1}(\phi_{x,x} + w_{,xx}) + \frac{\Phi_1}{E_1},\\
\varepsilon_y^0 &= \frac{F_{,xx} - \nu F_{,yy}}{E_1} - \frac{E_2}{E_1}\phi_{y,y} + \frac{cE_4}{E_1}(\phi_{y,y} + w_{,yy}) + \frac{\Phi_1}{E_1},\\
\gamma_{xy}^0 &= \frac{-2(1+\nu)}{E_1}F_{,xy} - \frac{E_2}{E_1}(\phi_{x,y} + \phi_{y,x}) + \frac{cE_4}{E_1}(\phi_{x,y} + \phi_{y,x} + 2w_{,xy}).
\end{aligned} \tag{19}$$

Substituting Eq. (19) into Eqs. (11, 12) yields

$$\begin{aligned}
M_x &= \frac{E_2}{E_1}F_{,yy} + \frac{E_1E_3 - E_2^2 + c(E_2E_4 - E_1E_5)}{E_1(1-\nu^2)}(\phi_{x,x} + \nu\phi_{y,y})\\
&\quad + \frac{c(E_2E_4 - E_1E_5)}{E_1(1-\nu^2)}(w_{,xx} + \nu w_{y,y}) + \frac{E_2\Phi_1 - E_1\Phi_2}{E_1(1-\nu)},\\
M_y &= \frac{E_2}{E_1}F_{,xx} + \frac{E_1E_3 - E_2^2 + c(E_2E_4 - E_1E_5)}{E_1(1-\nu^2)}(\phi_{y,y} + \nu\phi_{x,x})\\
&\quad + \frac{c(E_2E_4 - E_1E_5)}{E_1(1-\nu^2)}(w_{,yy} + \nu w_{x,x}) + \frac{E_2\Phi_1 - E_1\Phi_2}{E_1(1-\nu)},\\
M_{xy} &= -\frac{E_2}{E_1}F_{,xy} + \frac{E_1E_3 - E_2^2 + c(E_2E_4 - E_1E_5)}{2E_1(1+\nu)}(\phi_{x,y} + \phi_{y,x})\\
&\quad + \frac{c(E_2E_4 - E_1E_5)}{E_1(1+\nu)}w_{,xy},
\end{aligned} \tag{20}$$

$$\begin{aligned}
P_x &= \frac{E_4}{E_1}F_{,yy} + \frac{E_1E_5 - E_2E_4 + c(E_4^2 - E_1E_7)}{E_1(1-\nu^2)}(\phi_{x,x} + \nu\phi_{y,y})\\
&\quad + \frac{c(E_4^2 - E_1E_7)}{E_1(1-\nu^2)}(w_{,xx} + \nu w_{y,y}) + \frac{E_4\Phi_1 - E_1\Phi_4}{E_1(1-\nu)},\\
P_y &= \frac{E_4}{E_1}F_{,xx} + \frac{E_1E_5 - E_2E_4 + c(E_4^2 - E_1E_7)}{E_1(1-\nu^2)}(\phi_{y,y} + \nu\phi_{x,x})\\
&\quad + \frac{c(E_4^2 - E_1E_7)}{E_1(1-\nu^2)}(w_{,yy} + \nu w_{x,x}) + \frac{E_4\Phi_1 - E_1\Phi_4}{E_1(1-\nu)},\\
P_{xy} &= -\frac{E_4}{E_1}F_{,xy} + \frac{E_1E_5 - E_2E_4 + c(E_4^2 - E_1E_7)}{2E_1(1+\nu)}(\phi_{x,y} + \phi_{y,x})\\
&\quad + \frac{c(E_4^2 - E_1E_7)}{E_1(1+\nu)}w_{,xy}.
\end{aligned} \tag{21}$$

The substitution of Eq. (19) into the compatibility equation (7) and Eqs. (13, 20, 21) into Eqs. (17.2, 17.3, 17.4), yields a system of equations

$$\Delta\Delta F = -\frac{E_1}{R}w_{,xx} - \frac{E_1}{a}w_{,yy} + E_1(w_{,xy})^2 - E_1 w_{,xx}w_{,yy}, \tag{22}$$

$$A_1\Delta(\phi_{x,x}+\phi_{y,y})+A_2(\Delta\Delta w)+\frac{F_{,xx}}{R}+\frac{F_{,yy}}{a}+F_{,yy}w_{,xx}-2F_{,xy}w_{,xy}$$
$$+F_{,xx}w_{,yy}+q-K_1w+K_2\Delta w=0, \tag{23}$$
$$A_3(2\phi_{x,xxx}+\phi_{x,xyy}+\phi_{y,yxx}-\nu\phi_{x,xyy}+\nu\phi_{y,yxx})+A_4(w_{,xxxx}+w_{,xxyy})$$
$$+A_5(\phi_{x,x}+w_{,xx})=0, \tag{24}$$
$$A_3(2\phi_{y,yyy}+\phi_{y,yxx}+\phi_{x,xyy}-\nu\phi_{y,yxx}+\nu\phi_{x,xyy})+A_4(w_{,yyyy}+w_{,xxyy})$$
$$+A_5(\phi_{y,y}+w_{,yy})=0, \tag{25}$$

where

$$\begin{aligned}
&A_1=\frac{E_1E_3-E_2^2+c(E_2E_4-E_1E_5)}{E_1(1-\nu^2)},\ A_2=\frac{c(E_2E_4-E_1E_5)}{E_1(1-\nu^2)},\\
&A_3=\left[E_1E_3-E_2^2+2c(E_2E_4-E_1E_5)-c^2\left(E_4^2-E_1E_7\right)\right],\\
&A_4=2c\left[E_2E_4-E_1E_5-c\left(E_4^2-E_1E_7\right)\right],\ A_5=E_1(1-\nu)(-E_1+6cE_3-9c^2E_5),
\end{aligned} \tag{26}$$

Δ is the Laplace operator.

Equations (22, 23, 24) and (25) are four important governing equations used to investigate the nonlinear buckling of toroidal shells segment under external pressure surrounded by elastic foundation. Until now, there are no analytical investigations which have been reported in the literature on the postbuckling analysis of FGM thicker toroidal shells segment using Reddy's TSDT. *Therefore, the transformations and derivations to Eqs. (22–25) are one of the most important results in this work.*

3 Nonlinear buckling analysis

Suppose that the FGM toroidal shell segment is simply supported, freely movable (FM) in the axial direction and subjected to external pressure uniformly distributed q on the outer surface of shell. The associated boundary conditions are:

$$w=0,\ M_x=0,\ N_x=0,\ N_{xy}=0,\ \phi_y=0 \text{ at } x=0;\ x=L. \tag{27}$$

The deflection function w satisfying above boundary conditions on the average sense is assumed to be taken three terms as [4,42]

$$w=f_0+f_1\sin Mx\sin Ny+f_2\sin^2 Mx, \tag{28}$$

where $M=\frac{m\pi}{L}$; $N=\frac{n}{R}$; m is the number of half waves in axial direction, and n is the number of waves in circumferential direction of the shell. The first term of w in Eq. (28) represents the uniform deflection of points belonging to two butt-ends $x=0$ and $x=L$, the second term a linear buckling shape and the third a nonlinear buckling shape.

Substituting the expression of w from Eq. (28) into Eq. (22) yields:

$$\begin{aligned}
\frac{\Delta\Delta F}{E_1}=&\left[\left(\frac{M^2}{R}+\frac{N^2}{a}\right)f_1-M^2N^2f_1f_2\right]\sin Mx\sin Ny+M^2N^2f_1f_2\sin 3Mx\sin Ny\\
&+\left(\frac{M^2N^2}{2}f_1^2-\frac{2M^2}{R}f_2\right)\cos 2Mx+\frac{M^2N^2}{2}f_1^2\cos 2Ny.
\end{aligned} \tag{29}$$

The general solution of this equation can be found in the form

$$F=B_1\sin Mx\sin Ny+B_2\sin 3Mx\sin Ny+B_3\cos 2Mx+B_4\cos 2Ny+\frac{\sigma_{0y}h}{2}x^2, \tag{30}$$

where σ_{0y} is the negative average circumferential stress and

$$\begin{aligned}
B_1 &= \frac{E_1}{(M^2+N^2)^2}\left(\frac{M^2}{R}+\frac{N^2}{a}\right) f_1 - \frac{E_1 M^2 N^2}{(M^2+N^2)^2} f_1 f_2,\\
B_2 &= \frac{E_1 M^2 N^2}{(9M^2+N^2)^2} f_1 f_2,\\
B_3 &= \frac{E_1 N^2}{32M^2} f_1^2 - \frac{E_1}{8M^2 R} f_2,\\
B_4 &= \frac{E_1 M^2}{32N^2} f_1^2.
\end{aligned} \tag{31}$$

Substituting the expression of w from Eq. (28) into Eqs. (24) and (25), after some calculations, yields:

$$\begin{aligned}
&A_3(2\phi_{x,xxx}+\phi_{x,xyy}+\phi_{y,yxx}-\nu\phi_{x,xyy}+\nu\phi_{y,yxx})+A_5\phi_{x,x}\\
&\quad=\left[A_5-A_4(M^2+N^2)\right]M^2 f_1 \sin Mx \sin Ny + (8A_4M^4-2A_5M^2) f_2 \cos 2Mx,\\
&A_3(2\phi_{y,yyy}+\phi_{y,yxx}+\phi_{x,xyy}-\nu\phi_{y,yxx}+\nu\phi_{x,xyy})+A_5\phi_{y,y}\\
&\quad=\left[A_5-A_4(M^2+N^2)\right]N^2 f_1 \sin Mx \sin Ny.
\end{aligned} \tag{32}$$

The general solution of this equation can be found in the form

$$\begin{aligned}
\phi_{x,x} &= C_1 f_1 \sin Mx \sin Ny + C_2 f_2 \cos 2Mx,\\
\phi_{y,y} &= C_3 f_1 \sin Mx \sin Ny,
\end{aligned} \tag{33}$$

where

$$\begin{aligned}
C_1 &= \frac{A_4(M^2+N^2)-A_5}{2A_3(M^2+N^2)-A_5} M^2,\\
C_2 &= \frac{\left(8A_4M^4-2A_5M^2\right)}{A_5-8A_3M^2},\\
C_3 &= \frac{A_4(M^2+N^2)-A_5}{2A_3(M^2+N^2)-A_5} N^2.
\end{aligned} \tag{34}$$

Equations (33) and (34) are one of the novelties of this study.

In order to establish a load–defection curve, first of all, substituting Eqs. (28, 30) and (33) into Eq. (23) and then applying the Galerkin's method for the remaining equation in the ranges $0 \le y \le 2\pi R$ and $0 \le x \le L$, lead to

$$\frac{\sigma_{0y} h}{R} - K_1\left(f_0+\frac{1}{2}f_2\right)+q=0, \tag{35}$$

$$D_1 f_1^2 + D_2 f_1^2 f_2 + D_3 f_2 = 0, \tag{36}$$

$$D_4 f_1 - 2D_1 f_1 f_2 - D_2 f_1 f_2^2 + D_5 f_1^3 + \sigma_{0y} h N^2 f_1 = 0, \tag{37}$$

where

$$\begin{aligned}
D_1 &= \frac{E_1 M^2 N^2}{(M^2+N^2)^2}\left(\frac{M^2}{R}+\frac{N^2}{a}\right)+\frac{E_1 N^2}{8R},\\
D_2 &= -E_1 M^4 N^4\left(\frac{1}{(M^2+N^2)^2}+\frac{1}{(9M^2+N^2)^2}\right),\\
D_3 &= -\frac{1}{2}K_1 - 2M^2 K_2 + 4M^2 A_1 C_2 + 8M^4 A_2 - \frac{E_1}{2R^2},\\
D_4 &= (M^2+N^2)A_1(C_1+C_3) - (M^2+N^2)^2 A_2\\
&\quad + \frac{E_1}{(M^2+N^2)^2}\left(\frac{M^2}{R}+\frac{N^2}{a}\right)^2 + K_1 + K_2(M^2+N^2),\\
D_5 &= \frac{E_1(M^4+N^4)}{16}.
\end{aligned} \tag{38}$$

Furthermore, the toroidal shell segments have to also satisfy the circumferential closed condition [4–6,42] as

$$\int_0^{2\pi R}\int_0^{L} v_{,y}\mathrm{d}x\mathrm{d}y = \int_0^{2\pi R}\int_0^{L}\left(\varepsilon_y^0 + \frac{w}{R} - w_{,y}^2/2\right)\mathrm{d}x\mathrm{d}y = 0. \tag{39}$$

Using Eqs. (19), (28), (30) and (33), this integral leads to

$$\frac{\sigma_{0y}h}{E_1} - \frac{f_1^2 N^2}{8} + \frac{1}{R}\left(f_0 + \frac{1}{2}f_2\right) + \frac{\Phi_1}{E_1} = 0. \tag{40}$$

Solving Eqs. (35), (36) and (40) yields:

$$f_1^2 = \frac{-D_3 f_2}{D_1 + D_2 f_2}. \tag{41}$$

$$f_0 = -\frac{1}{2}f_2 + \frac{E_1 R N^2}{8(E_1 + K_1 R^2)}\left(\frac{-D_3 f_2}{D_1 + D_2 f_2}\right) + \frac{R^2}{E_1 + K_1 R^2}q - \frac{R\Phi_1}{E_1 + K_1 R^2}. \tag{42}$$

$$\sigma_{0y}h = -\frac{RE_1}{E_1 + K_1 R^2}q + \frac{K_1 E_1 R^2 N^2}{8(E_1 + K_1 R^2)}\left(\frac{-D_3 f_2}{D_1 + D_2 f_2}\right) - \frac{K_1 R^2 \Phi_1}{E_1 + K_1 R^2}. \tag{43}$$

Substituting Eqs. (41) and (43) into Eq. (37) leads to

$$q = \frac{D_4}{D_6} - \frac{2D_1}{D_6}f_2 - \frac{D_2}{D_6}f_2^2 + \frac{1}{D_6}\left(D_5 + \frac{K_1 E_1 R^2 N^4}{8(E_1 + K_1 R^2)}\right)\left(\frac{-D_3 f_2}{D_1 + D_2 f_2}\right) - \frac{K_1 R}{E_1}\Phi_1, \tag{44}$$

where

$$D_6 = \frac{RN^2 E_1}{E_1 + K_1 R^2}. \tag{45}$$

From Eq. (44), by taking $f_2 = 0$, the upper buckling stress of FGM toroidal shell segment can be determined by

$$q^{\mathrm{up}} = \frac{D_4}{D_6} - \frac{K_1 R}{E_1}\Phi_1. \tag{46}$$

Not to mention the influence of temperature, we have

$$q^{\mathrm{up}} = \frac{D_4}{D_6}. \tag{47}$$

Use the classical theory, with the same way as above, we obtain

$$q^{\mathrm{up}} = \frac{(M^2+N^2)^2\frac{E_1E_3 - E_2^2}{E_1(1-\nu^2)} + \left(\frac{M^2}{R} + \frac{N^2}{a}\right)^2\frac{E_1}{(M^2+N^2)^2} + K_1 + K_2(M^2+N^2)}{\frac{E_1 R N^2}{E_1 + K_1 R^2}}. \tag{48}$$

Minimizing Eqs. (46, 47 and 48) with respect to m and n, we will find the upper critical load.
If $q = 0$, from Eq. (44), we have

$$\frac{K_1 R}{E_1}\Phi_1 = \frac{D_4}{D_6} - \frac{2D_1}{D_6}f_2 - \frac{D_2}{D_6}f_2^2 + \frac{1}{D_6}\left(D_5 + \frac{K_1 E_1 R^2 N^4}{8\left(E_1 + K_1 R^2\right)}\right)\left(\frac{-D_3 f_2}{D_1 + D_2 f_2}\right). \tag{49}$$

Setting Eq. (16) into Eq. (49), after some calculations, we obtain

$$\Delta T = \frac{D_4}{D_8} - \frac{2D_1}{D_8}f_2 - \frac{D_2}{D_8}f_2^2 + \frac{1}{D_8}\left(D_5 + \frac{K_1 E_1 R^2 N^4}{8\left(E_1 + K_1 R^2\right)}\right)\left(\frac{-D_3 f_2}{D_1 + D_2 f_2}\right). \tag{50}$$

where

$$D_8 = \frac{K_1 R^2 N^2 \Phi_{10}}{E_1 + K_1 R^2}. \tag{51}$$

Taking $f_2 \to 0$, from Eq. (50) the thermal buckling load may be obtained as

$$\Delta T = \frac{D_4}{D_8} \tag{52}$$

Minimizing Eq. (52) with respect to m and n, we will find the critical value $\Delta T_{\rm cr}$.

From Eq. (28), it is obvious that the maximal deflection of shells

$$W_{\max} = f_0 + f_1 + f_2, \tag{53}$$

locates at $x = \frac{iL}{2m}$, $y = \frac{j\pi R}{2n}$ where i, j are odd integer numbers.

From Eqs. (41 and 42), the maximal deflection of shell can be determined by

$$W_{\max} = \frac{1}{2} f_2 + \frac{E_1 R N^2}{8(E_1 + K_1 R^2)} \left(\frac{-D_3 f_2}{D_1 + D_2 f_2} \right) + \frac{R^2}{E_1 + K_1 R^2} q + \left(\frac{-D_3 f_2}{D_1 + D_2 f_2} \right)^{1/2} - \frac{R\Phi_1}{E_1 + K_1 R^2}. \tag{54}$$

Combining Eq. (44) with Eq. (54), the static postbuckling load–maximal deflection curves of shells can be investigated.

4 Numerical results and discussion

4.1 Validation of the present study

To verify the accuracy of the present approach, two comparisons are considered below.

First comparison: Because present results are general than the ones of circular cylindrical shells, this part will give a comparison of the static postbuckling load–maximal deflection curve analyzed by us with results of Huang and Han [7] using the nonlinear large deflection theory and the Ritz energy method for an FGM cylindrical shell without foundation, under external pressure.

Figure 2, using Eqs. (44 and 54) with $a \to \infty$, shows that good agreements are obtained in this comparison.

Second comparison: Table 1 and Fig. 3 compare, respectively, the static critical load $q_{\rm cr}$ and the static postbuckling load–maximal deflection curves of this paper with the results given by Bich et al. [38] for FGM toroidal shell segment without foundation, under external pressure. The input parameters are taken as

$$E_{\rm c} = 370 \times 10^9\,{\rm Pa},\ E_{\rm m} = 70 \times 10^9\,{\rm Pa},\ k = 1,\ \nu = 0.3,\ R = 0.5\,{\rm m},\ a/R = 4,\ L/R = 2.$$

As can be seen, we also obtain good agreements in this comparison.

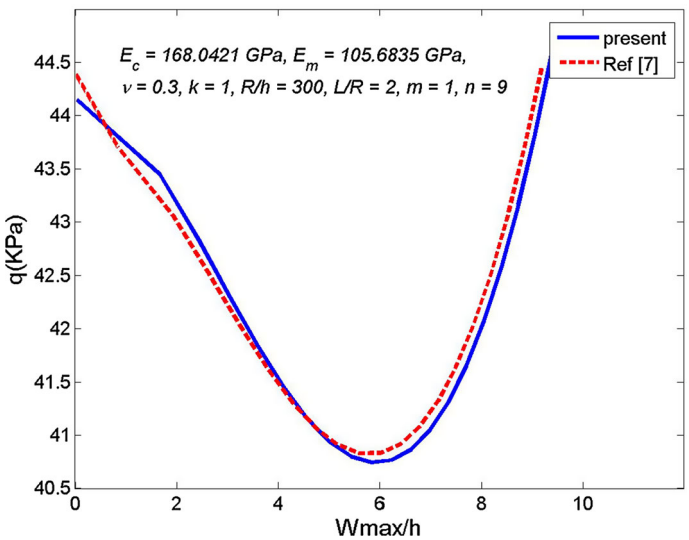

Fig. 2 Comparisons with results of [7]

Table 1 Comparisons on static critical loads q_{cr} (MPa) for FGM toroidal shell segment without foundation

R/h	q_{cr}(MPa)		
	Bich et al. [38]	Present study	% Error
80	5.7924 (1, 9)[a]	5.7834 (1, 9)	0.15
100	3.7635 (1, 10)	3.7591 (1, 10)	0.12
200	1.1550 (1, 14)	1.1544 (1, 14)	0.05
500	0.4493 (1, 23)	0.4492 (1, 23)	0.02

[a] The numbers in the parentheses denote the buckling mode (m, n)

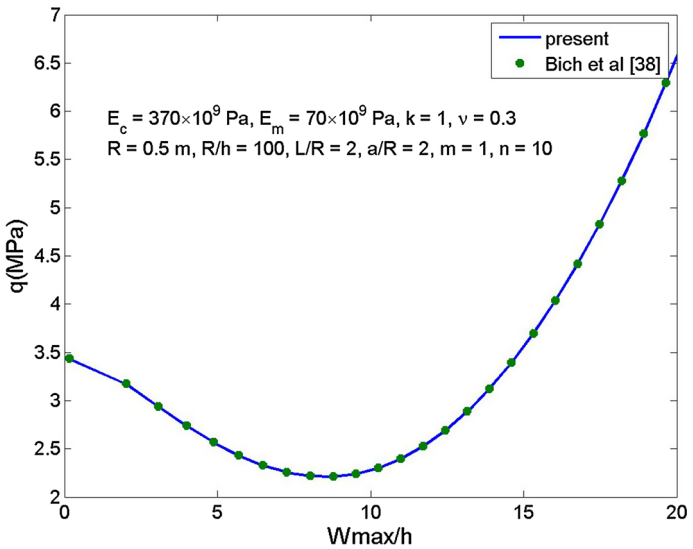

Fig. 3 Comparison on the static postbuckling load–maximal deflection curve

4.2 Significance of the use of the Reddy third-order shear deformation theory for thicker shells

In order to demonstrate the significance of the use of TSDT, a FGM toroidal shell segments subjected to uniform external pressure are considered with the following geometrical, material properties and foundation parameters as

$$E_c = 168.08 \times 10^9\,\text{Pa}, E_m = 105.69 \times 10^9\,\text{Pa}, k = 1, \nu = 0.3, R = 0.5\,\text{m}, a/R = 4, L/R = 2,$$
$$K_1 = 1.5 \times 10^7\,\text{N/m}^3, K_2 = 1.5 \times 10^5\,\text{N/m}.$$

The ratio R/h is chosen to be 10, 20, 30, 40, 50, 80, 100, 200 and 500.

Using Eqs. (47) and (48), results of upper critical loads based on the classical shell theory and Reddy's third-order shear deformation shell theory are given in Table 2.

As can be seen, for thin shells, the difference between the upper critical loads found from classical shell theory and TSDT is quite small. However, for the thicker shells, the difference is quite big. For example, from Table 2, with foundation, in comparison $q_{cr} = 0.41245$ MPa (based on CST) and $q_{cr} = 0.41241$ MPa (based on TSDT) corresponding to $R/h = 500$ (thin shell), the percentage error is 0.01 %, but when $R/h = 10$ (thick shell), the corresponding percentage error is 3.64%.

4.3 Results of nonlinear buckling analysis of FGM toroidal shell segments

In subsections below, consider a shell with geometrical and material properties as follows:

$$E_c = 168.08 \times 10^9\,\text{Pa}, E_m = 105.69 \times 10^9\,\text{Pa}, \alpha_c = 5.4 \times 10^{-6}\text{K}^{-1}, \alpha_m = 22.2 \times 10^{-6}\,\text{K}^{-1}, k = 1,$$
$$\nu = 0.3, R = 0.5\,\text{m}, R/h = 100, a/R = 4, L/R = 2, K_1 = 1.5 \times 10^7\,\text{N/m}^3, K_2 = 1.5 \times 10^5\,\text{N/m}.$$

Table 2 Upper critical loads found by CST and TSDT

R/h	With foundation			Without foundation		
	Be found by R-TSDT	Be found by CST	% Error	Be found by R-TSDT	Be found by CST	% Error
10	355.56778 (1, 4)[a]	368.51030 (1, 4)	3.64	354.55806 (1, 4)	367.49349 (1, 4)	3.52
20	73.87533 (1, 5)	74.75505 (1, 5)	1.2	73.16486 (1,5)	74.04361 (1, 5)	1.19
30	30.37287 (1, 6)	30.59558 (1, 6)	0.73	29.79414 (1,6)	30.01648 (1, 6)	0.74
40	16.52688 (1, 7)	16.62021 (1, 7)	0.56	16.02258 (1,7)	16.11570 (1, 7)	0.58
50	10.361813 (1, 7)	10.39251 (1, 7)	0.3	9.86534 (1,7)	9.89595 (1, 7)	0.31
80	4.04598 (1, 9)	4.05356 (1, 9)	0.19	3.62659 (1,9)	3.63414 (1, 9)	0.21
100	2.67021 (1, 10)	2.67394 (1, 10)	0.14	2.27326 (1,10)	2.27697 (1, 13)	0.16
200	0.89560 (1, 14)	0.89603 (1, 14)	0.05	0.54300 (1,13)	0.54332 (1, 13)	0.06
500	0.41241 (1, 23)	0.41245 (1, 23)	0.01	0.08403 (1,21)	0.08405 (1, 21)	0.02

[a] The numbers in the parentheses denote the buckling mode (m, n)

Table 3 Effects of temperature field on critical load

ΔT(K)	Convex shell $(a/R = 4)$ q_{cr} (MPa)	Concave shell $(a/R = -4)$ q_{cr} (MPa)
0	2.6702 (1, 10)[a]	1.3305 (2, 6)
300	2.6406 (1, 10)	1.3009 (2, 6)
600	2.6110 (1, 10)	1.2713 (2, 6)
900	2.5814 (1, 10)	1.2417 (2, 6)

[a] The numbers in the parentheses denote the buckling mode (m, n)

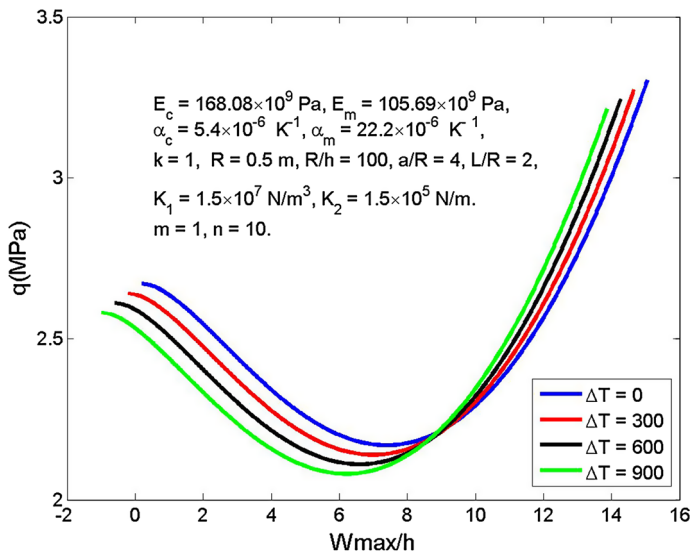

Fig. 4 Effects of temperature field on $(q-W_{\max}/h)$ curves of FGM convex shell

4.3.1 Effect of temperature field

The effect of a uniform temperature rise on the buckling and postbuckling is considered in this section. Basing on Eqs. (44, 46) and (54), the critical load and postbuckling paths $(q-W_{\max}/h)$ may be determined. The results are given in Table 3, Figs. 4 and 5. It can be seen that the upper critical load of shell reduces when ΔT increases. For example, from Table 3, with a convex shell, the upper critical load $q_{cr} = 2.6702$MPa corresponding to $\Delta T = 0$K is larger than the upper critical load $q_{cr} = 2.6406$ MPa corresponding to $\Delta T = 300$(K) by about 1.12%. For a concave shell, this difference is about 2.2%.

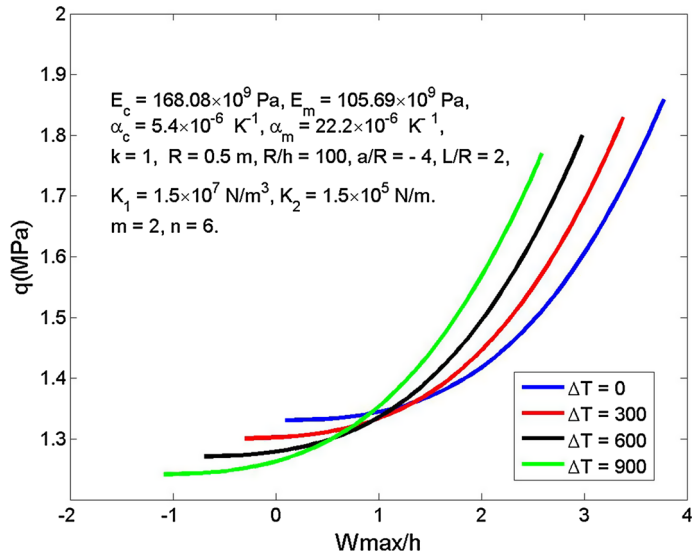

Fig. 5 Effects of temperature field on $(q-W_{\max}/h)$ curves of FGM concave shell

Table 4 Effects of volume fraction indexes on critical load and critical value $\Delta T_{\rm cr}$

k	Convex shell $(a/R=4)$		Concave shell $(a/R=-4)$	
	$q_{\rm cr}$ (MPa)	$\Delta T_{\rm cr}$ (K)	$q_{\rm cr}$ (MPa)	$\Delta T_{\rm cr}$ (K)
0	3.2158 (1, 10)[a]	79403 (1, 10)	1.5125 (2, 6)	37,345 (2, 6)
0.2	3.0148 (1, 10)	49822 (1, 10)	1.4411 (2,6)	23,815 (2, 6)
0.5	2.8309 (1, 10)	35593 (1, 10)	1.3793 (2,6)	17,342 (2, 6)
1	2.6702 (1, 10)	27050 (1, 10)	1.3305 (2,6)	13,478 (2, 6)
5	2.4022 (1, 10)	17009 (1, 10)	1.2628 (2,6)	8942 (2, 6)
∞	2.1704 (1, 10)	13035 (1,10)	1.1743 (2, 6)	7053 (2, 6)

[a] The numbers in the parentheses denote the buckling mode (m, n)

4.3.2 Effects of material properties

Based on Eqs. (44, 46, 52) and (54), with the database given in Sect. 4.2, the effects of volume fraction indexes on critical load, critical value $\Delta T_{\rm cr}$ and $(q-W_{\max}/h)$ curves are considered. Results are shown in Table 4, Figs. 6 and 7. As expected, both critical load and critical value $\Delta T_{\rm cr}$ are very much reduced as k increases. For example, with convex shell, when k increases from 0.2 to 1, the upper critical load decreases from 3.0148 MPa to 2.6702 MPa (about 11.4%) and the critical value $\Delta T_{\rm cr}$ decreases from 49822 to 27050 K correspondingly (about 45.7%). This property corresponds to the real property of material, because the higher value of k corresponds to a metal richer shell which usually has less stiffness and less thermostability than a ceramic richer one. Moreover, the load-bearing capacity of FGM concave toroidal shells is lower than that of FGM convex toroidal shells. For example, with $k=1$, the upper critical load of a convex shell is bigger than upper critical load of a concave shell by about 2.05 times.

4.3.3 Effects of the ratio R/h

Information in Table 5, Figs. 8 and 9 shows that both critical load and critical value $\Delta T_{\rm cr}$ are very sensitive with the change of the ratio R/h; buckling load and critical value $\Delta T_{\rm cr}$ decrease markedly with the increase of this ratio. For example, with a convex shell, the upper critical load $q^{\rm up}=4.0460$MPa corresponding to $R/h=80$ is higher than the upper critical load corresponding to $R/h=100$ by about 1.5 times. It is shown that the similar behavior is observed for convex and concave shells.

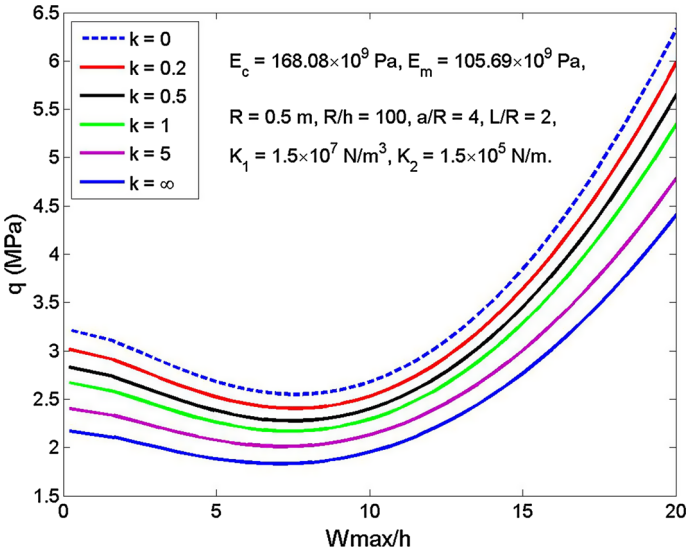

Fig. 6 Effects of volume fraction indexes on $(q-W_{\max}/h)$ curves of FGM convex shell

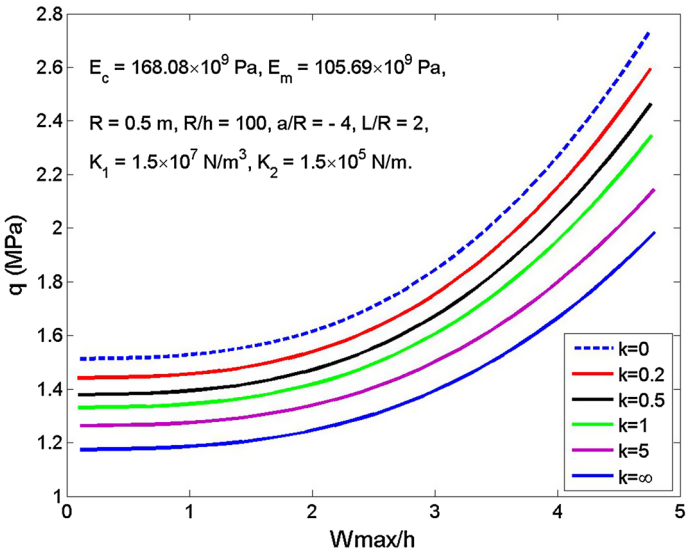

Fig. 7 Effects of volume fraction indexes on $(q-W_{\max}/h)$ curves of FGM concave shell

Table 5 Effects of the ratio R/h on critical load and critical value ΔT_{cr}

R/h	Convex shell $(a/R=4)$		Concave shell $(a/R=-4)$	
	q_{cr} (MPa)	ΔT_{cr} (K)	q_{cr} (MPa)	ΔT_{cr} (K)
80	4.0460 (1, 9)[a]	40,987 (1, 9)	1.6424 (1, 3)	16,638 (1, 3)
100	2.6702 (1, 10)	27,050 (1, 10)	1.3305 (2, 6)	13,478 (2, 6)
200	0.8956 (1, 14)	9073 (1, 14)	0.6523 (2, 7)	6608 (2, 7)
500	0.4124 (1, 23)	4178 (1, 23)	0.4097 (1, 22)	4150 (1, 22)

[a] The numbers in the parentheses denote the buckling mode (m, n)

4.3.4 Effects of the ratio L/R

Effects of the ratio L/R on the critical load and postbuckling curves of a shell are represented in Table 6, Figs. 10 and 11. As can be observed, for a convex shell, both the critical load and the critical value ΔT_{cr} are reduced with the increase of the ratio L/R, but not for a concave shell.

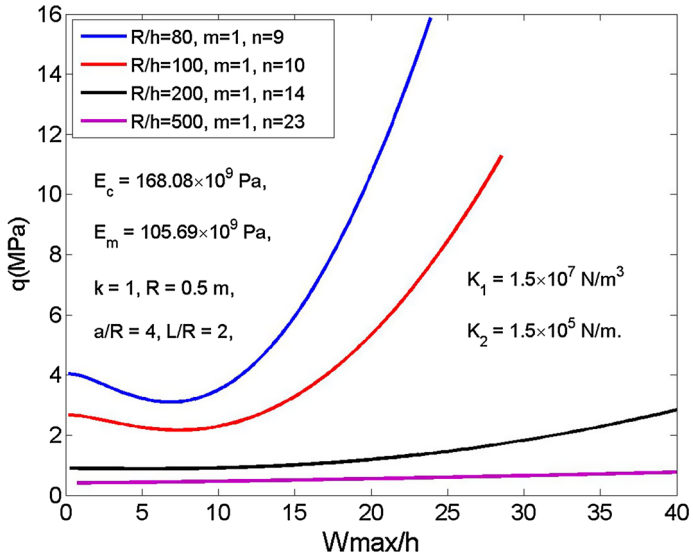

Fig. 8 Effects of the ratio R/h on $(q-W_{\max}/h)$ curves of FGM convex shell

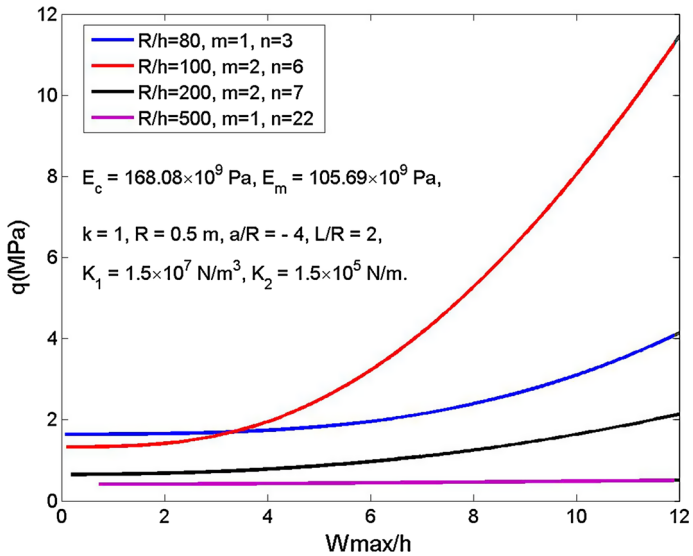

Fig. 9 Effects of the ratio R/h on $(q-W_{\max}/h)$ curves of FGM concave shell

Table 6 Effects of the ratio L/R on critical load and critical value $\Delta T_{\rm cr}$

L/R	Convex shell $(a/R=4)$		Concave shell $(a/R=-4)$	
	$q_{\rm cr}$ (MPa)	$\Delta T_{\rm cr}$ (K)	$q_{\rm cr}$ (MPa)	$\Delta T_{\rm cr}$ (K)
2	2.6702 (1, 10)[a]	27050 (1, 10)	1.3305 (2, 6)	13,478 (2, 6)
4	2.5214 (1, 10)	25543 (1,10)	1.1611 (3, 5)	11,762 (3, 5)
6	2.4871 (1, 9)	25195 (1,9)	1.2080 (5, 5)	12,238 (5, 5)
8	2.4742 (1, 9)	25065 (1,9)	1.1552 (5, 4)	11,703 (5, 4)

[a] The numbers in the parentheses denote the buckling mode (m, n)

4.3.5 Effects of longitudinal curvature radius a

Table 7, Figs. 12 and 13 depict the effects of the ratio $a/R = (\pm 2; \pm 4; \pm 6; \pm 8)$ on the nonlinear behavior of the shell, where the positive sign corresponds to a convex shell and the negative sign to a concave shell, respectively. It is shown that the buckling load decreases markedly with an increase of the ratio a/R and the

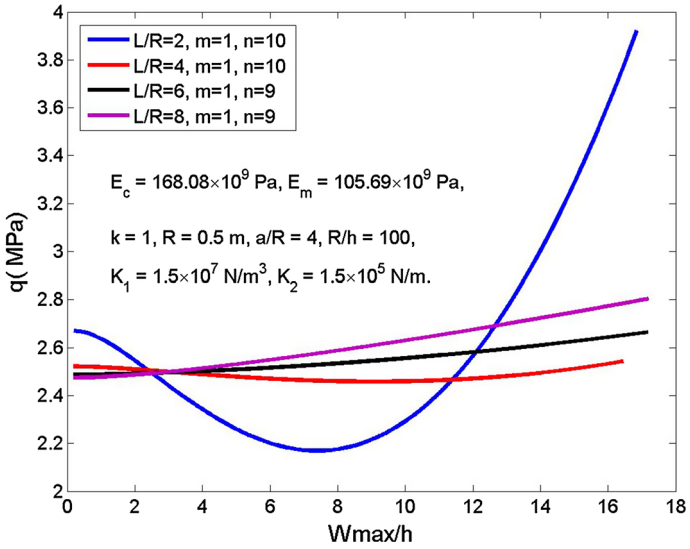

Fig. 10 Effects of the ratio L/R on $(q-W_{\max}/h)$ curves of FGM convex shell

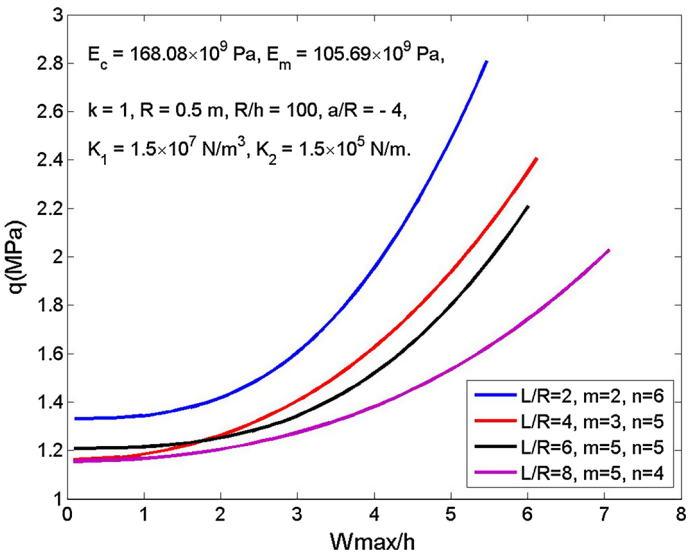

Fig. 11 Effects of the ratio L/R on $(q-W_{\max}/h)$ curves of FGM concave shell

Table 7 Effects of the ratio a/R on critical load and critical value ΔT_{cr}

Convex shell			Concave shell		
a/R	q_{cr} (MPa)	ΔT_{cr} (K)	a/R	q_{cr} (MPa)	ΔT_{cr} (K)
2	4.5901 (1, 13)[a]	46499 (1, 13)	−2	1.6374 (2, 5)	16,588 (2, 5)
4	2.6702 (1, 10)	27050 (1, 10)	−4	1.3305 (2, 6)	13,478 (2, 6)
6	2.0886 (1, 9)	21158 (1, 9)	−6	1.0934 (1, 4)	11,076 (1, 4)
8	1.8178 (1, 8)	18415 (1, 9)	−8	1.0381 (1, 5)	10,516 (1, 5)

[a] The numbers in the parentheses denote the buckling mode (m, n)

critical load is very sensitive with the change of the ratio a/R. This behavior is common to both convex and concave shells.

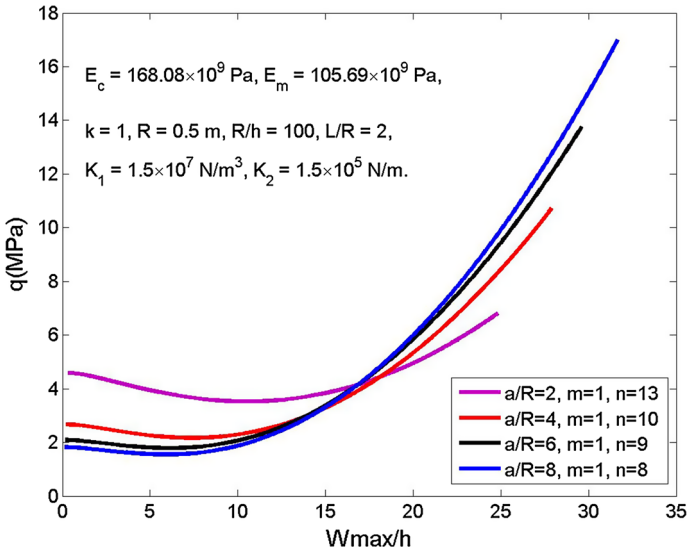

Fig. 12 Effects of the ratio a/R on $(q-W_{\max}/h)$ curves of FGM convex shell

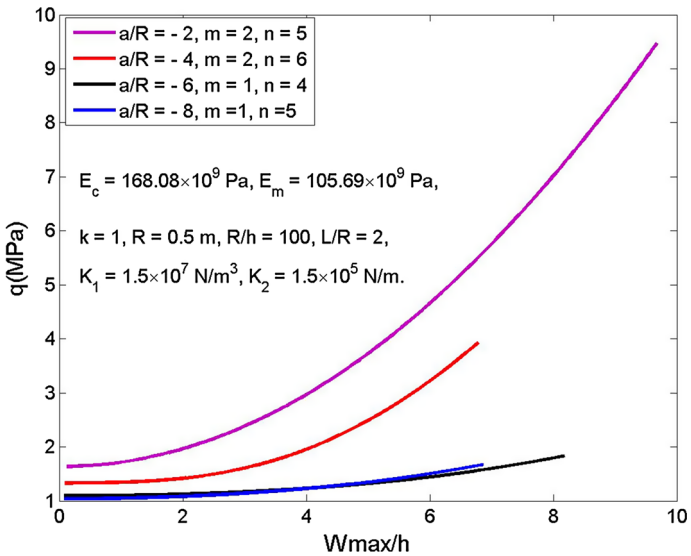

Fig. 13 Effects of the ratio a/R on $(q-W_{\max}/h)$ curves of FGM concave shell

Table 8 Effects of elastic foundation parameters on critical load of FGM convex shell and concave shell

Elastic foundation parameters	q_{cr}(MPa)	
	Convex shell $(a/R=4)$	Concave shell $(a/R=-4)$
$K_1=0\,\mathrm{N/m^3}$, $K_2=0\,\mathrm{N/m}$	2.2733 (1, 10)[a]	0.2346 (1, 3)
$K_1=1.5\times10^7\,\mathrm{N/m^3}$, $K_2=0\,\mathrm{N/m}$	2.3611 (1, 10)	0.9462 (2, 6)
$K_1=0\,\mathrm{N/m^3}$, $K_2=1.5\times10^5\,\mathrm{N/m}$	2.5806 (1, 10)	0.6168 (1, 3)
$K_1=1.5\times10^7\,\mathrm{N/m^3}$, $K_2=1.5\times10^5\,\mathrm{N/m}$	2.6702 (1, 10)	1.3305 (2, 6)

[a] The numbers in the parentheses denote the buckling mode (m, n)

4.3.6 Effects of elastic foundation parameters

Table 8, Figs. 14 and 15 show the influence of the foundation parameters on the critical load and $(q-W_{\max}/h)$ curves of the FGM toroidal shell. As can be seen, with concave shells, the Winkler foundation modulus has

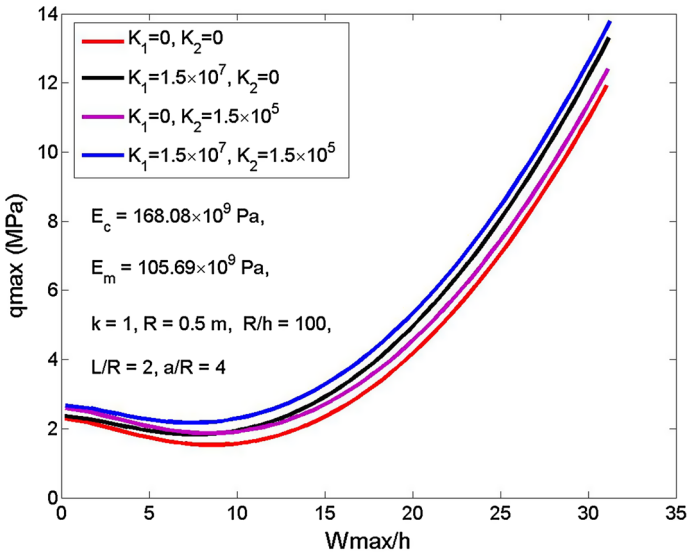

Fig. 14 Effects of elastic foundation parameters on $(q-W_{\max}/h)$ curves of FGM convex shell

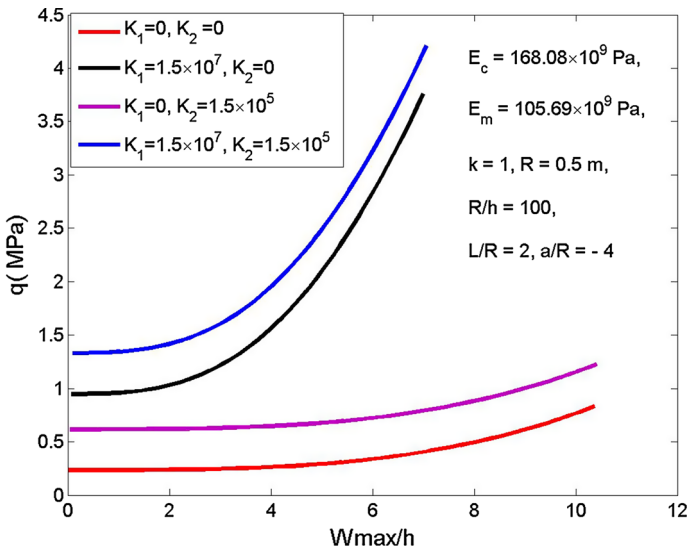

Fig. 15 Effects of elastic foundation parameters on $(q-W_{\max}/h)$ curves of FGM concave shell

a great influence on the critical load, but the shear layer foundation stiffness of the Pasternak model less influential.

5 Concluding remarks

In this paper, FGM toroidal shell segments surrounded by elastic foundation and subjected to uniform external pressure are considered.

An analytical approach to investigate the nonlinear buckling and postbuckling behavior of shells based on the Reddy's third-order shear deformation shell theory is presented.

An approximate three-term solution of deflection including the linear and nonlinear buckling shape is more correctly chosen.

Closed-form expressions to determine critical buckling loads and nonlinear postbuckling load–deflection curves are obtained using Galerkin's method.

For thin shells, the difference between the upper critical loads found from CST and TSDT is quite small, so the classical shell theory can be used to study the stability of thin shells. However, for thicker shells, the difference is quite big and the use of TSDT to analyze the nonlinear stability of toroidal shell segments is necessary and more suitable.

Parameters as temperature, geometrical dimension, buckling modes, volume fraction index and foundation parameters strongly affect the buckling and postbuckling of shells.

Acknowledgements This research is funded by Vietnam National Foundation for Science and Technology Development (NAFOSTED) under Grant No. 107.02-2015.11.

References

1. Batra, R.C.: Torsion of a functionally graded cylinder. AIAA J. **44**, 1363–1365 (2006)
2. Wang, H.M., Liu, C.B., Ding, H.J.: Exact solution and transient behavior for torsional vibration of functionally graded finite hollow cylinders. Acta Mech. Sin. **25**, 555–563 (2009)
3. Shen, H.S.: Torsional buckling and postbuckling of FGM cylindrical shells in thermal environments. Int. J. Non-Linear Mech. **44**, 644–657 (2009)
4. Huang, H., Han, Q.: Nonlinear buckling of torsion-loaded functionally graded cylindrical shells in thermal environment. Eur. J. Mech. A Solids. **29**, 42–48 (2010)
5. Huang, H., Han, Q.: Nonlinear elastic buckling and postbuckling of axially compressed functionally graded cylindrical shells. Int. J. Mech. Sci. **51**, 500–507 (2009)
6. Huang, H., Han, Q.: Nonlinear buckling and postbuckling of heated functionally graded cylindrical shells under combined axial compression and radial pressure. Int. J. Non-Linear Mech. **44**, 209–218 (2009)
7. Huang, H., Han, Q.: Research on nonlinear postbuckling of FGM cylindrical shells under radial loads. Compos. Struct. **92**, 1352–1357 (2010)
8. Huang, H., Han, Q.: Nonlinear dynamic buckling of functionally graded cylindrical shells subjected to a time-dependent axial load. Compos. Struct. **92**, 593–598 (2010)
9. Sofiyev, A., Schnack, H.E.: The stability of functionally graded cylindrical shells under linearly increasing dynamic torsional loading. Eng. Struct. **26**, 1321–1331 (2004)
10. Najafizadeh, M.M., Hasani, A., Khazaeinejad, P.: Mechanical stability of functionally graded stiffened cylindrical shells. Appl. Math. Model. **33**, 1151–1157 (2009)
11. Bich, D.H., Dung, D.V., Nam, V.H.: Nonlinear dynamic analysis of eccentrically stiffened imperfect functionally graded doubly curved thin shallow shells. Compos. Struct. **96**, 384–395 (2013)
12. Bich, D.H., Dung, D.V., Nam, V.H., Phuong, N.T.: Nonlinear static and dynamic buckling analysis of imperfect eccentrically stiffened functionally graded circular cylindrical thin shells under axial compression. Int. J. Mech. Sci. **74**, 190–200 (2013)
13. Dung, D.V., Hoa, L.K.: Research on nonlinear torsional buckling and postbuckling of eccentrically stiffened functionally graded thin circular cylindrical shells. Compos. Part B **51**, 300–309 (2013)
14. Dung, D.V., Hoa, L.K.: Nonlinear buckling and postbuckling analysis of eccentrically stiffened functionally graded circular cylindrical shells under external pressure. Thin-Walled Struct. **63**, 117–124 (2013)
15. Sheng, G.G., Wang, X.: Thermal vibration, buckling and dynamic stability of functionally graded cylindrical shells embedded in an elastic medium. J. Reinf. Plastic. Compos. **27**, 117–134 (2008)
16. Shen, H.S.: Postbuckling of shear deformable FGM cylindrical shells surrounded by an elastic medium. Int. J. Mech. Sci. **51**, 372–383 (2009)
17. Shen, H.S., Yang, J., Kitipornchai, S.: Postbuckling of internal pressure loaded FGM cylindrical shells surrounded by an elastic medium. Eur. J. Mech. A/Solids. **29**, 448–460 (2010)
18. Sofiyev, A.H., Avcar, M.: The stability of cylindrical shells containing a FGM layer subjected to axial load on the Pasternak foundation. Engineering **2**, 228–236 (2010)
19. Sofiyev, A.H., Kuruoglu, N.: Torsional vibration and buckling of the cylindrical shell with functionally graded coatings surrounded by an elastic medium. Compos. Part B **45**, 1133–1142 (2013)
20. Najafov, A.M., Sofiyev, A.H., Kuruoglu, N.: Torsional vibration and stability of functionally graded orthotropic cylindrical shells on elastic foundations. Meccanica **48**, 829–840 (2013)
21. Bagherizadeh, E., Kiani, Y., Eslami, M.R.: Mechanical buckling of functionally graded material cylindrical shells surrounded by Pasternak elastic foundation. Compos. Struct. **93**, 3063–3071 (2011)
22. Akbari, M., Kiani, Y., Eslami, M.R.: Thermal buckling of temperature-dependent FGM conical shells with arbitrary edge supports. Acta. Mech. **226**, 897–915 (2015)
23. Bich, D.H., Tung, H.V.: Nonlinear axisymmetric response of functionally graded shallow spherical shells under uniform external pressure including temperature effects. Int. J. Non-linear. Mech. **46**, 1195–1204 (2011)
24. Dung, D.V., Nam, V.H.: Nonlinear dynamic analysis of eccentrically stiffened functionally graded circular cylindrical thin shells under pressure and surrounded by an elastic medium. Eur. J. Mech. A/Solids. **46**, 42–53 (2013)
25. Stein, M., McElman, J.A.: Buckling of segments of toroidal shells. AIAA. J. **3**, 1704–1709 (1965)
26. Hutchinson, J.W.: Initial postbuckling behavior of toroidal shell segments. Int. J. Solids. Struct. **3**, 97–115 (1967)
27. Parnell, T.K.: Numerical improvement of asymptotic solutions for shells of revolution with application to toroidal shell segments. Comput. Struct. **16**(1–4), 109–117 (1983)
28. Guodong, C.: Exact solutions of toroidal shells in pressure vessels and piping. Int. J. Press. Vessel Pip. **19**, 101–115 (1985)
29. Wang, Anwen, Zhang, Wei: Asymptotic solution for buckling toroidal shells. Int. J. Press. Vessel Pip. **45**, 61–72 (1991)

30. Zhang, R.J.: Toroidal shells under nonsymmetric loading. Int. J. Solids Struct. **31**(19), 2735–2750 (1994)
31. Zhu, F.: Vibration and stability analysis of toroidal shells conveying fluid. J. Sound Vib. **183**(2), 197–208 (1995)
32. Blachut, J., Jaiswal, O.R.: On buckling of toroidal shells under external pressure. Comput. Struct. **77**, 233–251 (2000)
33. Kuznetsov, V.V., Levyakov, S.V.: Nonlinear pure bending of toroidal shells of arbitrary cross-section. Int. J Solids Struct. **38**, 7343–7354 (2001)
34. Ming, R.S., Pan, J., Norton, M.P.: Free vibrations of elastic circular toroidal shells. Appl. Acoust. **63**, 513–528 (2002)
35. Buchanan, G.R., Liu, Y.J.: An analysis of the free vibration of thick-walled isotropic toroidal shells. Int. J. Mech. Sci. **47**, 277–292 (2005)
36. Asratyan, M.G., Gevorgyan, R.S.: Mixed boundary-value problems of thermoelasticity anisotropic-in-plane inhomogeneous toroidal shells. J. Appl. Math. Mech. **74**, 306–312 (2010)
37. Tornabene, F., Viola, E.: Static analysis of functionally graded doubly-curved shells and panels of revolution. Meccanica **48**, 901–930 (2013)
38. Bich, D.H., Ninh, D.G., Thinh, T.I.: Non-linear buckling analysis of FGM toroidal shell segments filled inside by an elastic medium under external pressure loads including temperature effects. Compos. Part B. **87**, 75–919 (2016)
39. Brush, D.O., Almroth, B.O.: Buckling of Bars, Plates and Shells. Mc Graw-Hill, New York (1975)
40. Reddy, J.N.: Mechanics of Laminated Composite Plates and Shells, Theory and Analysis. CRS Press, Boca Raton (2004)
41. Pasternak, P.L.: On a new method of analysis of an elastic foundation by mean of two foundation constan, Gos Izd Lit Po Stroit Arkh. Moscow, URSS (1954)
42. Volmir, A.S.: Stability of elastic systems, Science Edition. Moscow (1963)